

A radius of curvature approach to the Kolmogorov–Sinai entropy of dilute hard particles in equilibrium

Astrid S de Wijn¹ and Henk van Beijeren²

¹ Institute for Molecules and Materials, Faculty of Science, Radboud University Nijmegen, Heyendaalseweg 135, 6525 AJ Nijmegen, The Netherlands

² Institute for Theoretical Physics, Utrecht University, Leuvenlaan 4, 3584 CE, Utrecht, The Netherlands

E-mail: A.S.deWijn@science.ru.nl and H.vanBeijeren@uu.nl

Received 19 May 2011

Accepted 14 July 2011

Published 24 August 2011

Online at stacks.iop.org/JSTAT/2011/P08012

doi:[10.1088/1742-5468/2011/08/P08012](https://doi.org/10.1088/1742-5468/2011/08/P08012)

Abstract. We consider the Kolmogorov–Sinai entropy for dilute gases of N hard disks or spheres. This can be expanded in density as $h_{KS} \propto nN[\ln na^d + B + O(na^d) + O(1/N)]$, with a the diameter of the sphere or disk, n the density, and d the dimensionality of the system. We estimate the constant B by solving a linear differential equation for the approximate distribution of eigenvalues of the inverse radius of curvature tensor. We compare the resulting values of B both to previous estimates and to existing simulation results, finding very good agreement with the latter. Also, we compare the distribution of eigenvalues of the inverse radius of curvature tensor resulting from our calculations to new simulation results. For most of the spectrum the agreement between our calculations and the simulations again is very good.

Keywords: dynamical processes (theory), stationary states, kinetic theory of gases and liquids, molecular dynamics

Contents

1. Introduction	2
2. Lyapunov exponents and dynamics of hard spheres in tangent space	3
3. The radius of curvature tensor	5
3.1. KS entropy and the inverse ROC tensor	5
3.2. Dynamics of the inverse radius of curvature tensor	7
3.3. The eigenvalue distribution at low densities	8
4. The distribution of eigenvalues of the inverse radius of curvature tensor	8
4.1. The first approximation scheme	8
4.2. The second approximation scheme	10
5. Results and discussion	12
5.1. Comparing approximation schemes	13
5.2. The distribution of eigenvalues from a simulation	16
6. Conclusions	16
Acknowledgments	17
Appendix A. Eigenvalues of a submatrix	17
Appendix B. Narrowing of the eigenvalue spectrum	18
References	19

1. Introduction

It is generally believed that the approach to equilibrium of a typical many-particle system, such as a gas or liquid, will depend on its dynamical properties. Specifically, the more chaotic the system, the more rapidly its approach to (at least local) equilibrium will proceed. Furthermore, the apparent randomness of these systems, in spite of their fully deterministic microscopic behavior (at least for classical systems), has also been attributed to the chaotic nature of their dynamics. Discussions of this can be found in e.g. books by Dorfman [1] and Gaspard [2] and review papers by Van Zon *et al* [3, 4]. A very common and generally used measure of chaos is the Kolmogorov–Sinai entropy, which we will denote by h_{KS} . In systems which are closed, the Kolmogorov–Sinai entropy h_{KS} equals the sum of all positive Lyapunov exponents, the average rates over very long times of divergence (or convergence) of infinitesimal perturbations. It describes the rate at which the system produces information about its phase-space trajectories, or equivalently about the distribution of density over phase space in some ensemble. In systems with escape, the Kolmogorov–Sinai entropy has also been connected to transport coefficients [5]–[8]. In such systems it is no longer equal to the sum of all positive Lyapunov exponents.

Chaotic properties such as the Lyapunov spectrum of systems of low [8]–[11] as well as high [12] dimensionality, such as moving hard spheres or disks, have been studied

frequently. Extensive simulation work has been done on their Lyapunov spectra [13]–[15], and for low densities analytic calculations have been done for the largest Lyapunov exponent [3], [16]–[18], the Kolmogorov–Sinai entropy [11, 16] and for the smallest positive Lyapunov exponents [19, 20]. Analytic methods employing kinetic theory have been applied to calculate chaotic properties. Agreement between analytic calculations and numerical results is generally good, but with respect to the KS entropy there is one notorious exception, which is the central issue of the present paper.

In this paper we consider a system consisting of N hard, spherical particles, of diameter a , at small number density n , in d dimensions ($d = 2, 3$). We calculate the Kolmogorov–Sinai entropy in the low-density approximation, where it is expected to behave as [11]

$$h_{\text{KS}} = N\bar{v}A \left[-\ln(na^d) + B + O(na^d) + O\left(\frac{1}{N}\right) \right]. \quad (1)$$

The constant A has been calculated by Van Beijeren *et al* in [11], but the results found there for B were unsatisfactory.

In this paper we present a more successful calculation of B , through the distribution of eigenvalues of the inverse radius of curvature tensor. The calculation presented here differs from that presented by De Wijn in [21], in that it is far more elegant and less cumbersome and the agreement of the results with values found in simulations is better. On the other hand, the calculation here is less systematic and it is not clear how to apply the results of this paper to calculating specific Lyapunov exponents, as can be done [22] with the results of [21].

The paper is organized as follows. In section 2 we introduce Lyapunov exponents and review the properties of hard-sphere dynamics in tangent space (the space in which the dynamics is described, of infinitesimal deviations between nearby trajectories in phase space). In section 3 we introduce the radius of curvature tensor and its inverse, relate the KS entropy to the time average of the trace of the inverse radius of curvature tensor and investigate the dynamics of these tensors both during free flight and in collisions. In 4 we present two approximate calculations of the average distribution of the eigenvalues of the inverse radius of curvature tensor. In section 5 we compare the results of these calculations to those of numerical simulations and we also compare the resulting values for the coefficient B in equation (1) to those obtained in simulations and in previous calculations. Finally, in section 6 we present our conclusions.

2. Lyapunov exponents and dynamics of hard spheres in tangent space

This section is an abbreviated version of similar sections in [20, 21]. It appears here to make this paper more self-contained. For more details the reader may also consult [14]. Consider a system with an \mathcal{N} -dimensional phase space Γ . At time $t = 0$ the system is at an initial point γ_0 in this space. It evolves with time, according to $\gamma(\gamma_0, t)$. If the initial conditions are perturbed infinitesimally, by $\delta\gamma_0$, the system evolves along an infinitesimally different path $\gamma + \delta\gamma$, which can be specified by

$$\delta\gamma(\gamma_0, t) = M_{\gamma_0}(t) \cdot \delta\gamma_0, \quad (2)$$

with the matrix $\mathbf{M}_{\gamma_0}(t)$ defined by

$$\mathbf{M}_{\gamma_0}(t) = \frac{d\gamma(\gamma_0, t)}{d\gamma_0}. \quad (3)$$

The Lyapunov exponents are the possible average rates of growth or shrinkage of such perturbations, i.e.,

$$\lambda_i = \lim_{t \rightarrow \infty} \frac{1}{t} \ln |\mu_i(t)|, \quad (4)$$

where $\mu_i(t)$ is the i th eigenvalue of $\mathbf{M}_{\gamma_0}(t)$. For ergodic systems, the Lyapunov exponents are expected to be the same for almost all initial conditions. For each exponent there is a corresponding eigenvector of $\mathbf{M}_{\gamma_0}(t)$.

For a classical system of hard spheres without internal degrees of freedom, the phase space and tangent space may be represented by the positions and velocities of all particles and their infinitesimal deviations,

$$\gamma_i = (\mathbf{r}_i, \mathbf{v}_i), \quad (5)$$

$$\delta\gamma_i = (\delta\mathbf{r}_i, \delta\mathbf{v}_i), \quad (6)$$

where i runs over all particles and γ_i and $\delta\gamma_i$ are the contributions of particle i to γ and $\delta\gamma$.

In the case of a purely Hamiltonian system, such as the one under consideration here, hard spheres with only the hard-particle interaction, the dynamics of the system are completely invariant under time reversal. Together with Liouville's theorem, which states that phase-space volumes are invariant under the flow, this leads to the conjugate pairing rule [23, 24], i.e. for every positive Lyapunov exponent there is a negative exponent of equal absolute value. In systems which are time reversal invariant, but do not satisfy Liouville's theorem, the conditions for and the form of the conjugate pairing rule are somewhat different [17].

The system under consideration here has only hard-core interactions. Consequently, the evolution in phase space consists of an alternating sequence of free flights and collisions.

During free flights the particles do not interact and the positions change linearly with the velocities. The components of the tangent-space vector accordingly transform to

$$\begin{pmatrix} \delta\mathbf{r}'_i \\ \delta\mathbf{v}'_i \end{pmatrix} = \begin{pmatrix} \mathbf{1} & (t - t_0)\mathbf{1} \\ 0 & \mathbf{1} \end{pmatrix} \cdot \begin{pmatrix} \delta\mathbf{r}_i \\ \delta\mathbf{v}_i \end{pmatrix}, \quad (7)$$

in which $\mathbf{1}$ is the $d \times d$ identity matrix.

In a collision between particles i and j momentum is exchanged between the colliding particles along the collision normal, $\hat{\boldsymbol{\sigma}} = (\mathbf{r}_i - \mathbf{r}_j)/a$, as shown in figure 1. The other particles do not interact. For convenience we switch to relative and center of mass coordinates, $\delta\mathbf{r}_{ij} = \delta\mathbf{r}_i - \delta\mathbf{r}_j$, $\delta\mathbf{R}_{ij} = (\delta\mathbf{r}_i + \delta\mathbf{r}_j)/2$, $\delta\mathbf{v}_{ij} = \delta\mathbf{v}_i - \delta\mathbf{v}_j$, and $\delta\mathbf{V}_{ij} = (\delta\mathbf{v}_i + \delta\mathbf{v}_j)/2$. We find [16, 25]

$$\delta\mathbf{r}'_{ij} = \delta\mathbf{r}_{ij} - 2\mathbf{S} \cdot \delta\mathbf{r}_{ij}, \quad (8)$$

$$\delta\mathbf{R}'_{ij} = \delta\mathbf{R}_{ij}, \quad (9)$$

$$\delta\mathbf{v}'_{ij} = \delta\mathbf{v}_{ij} - 2\mathbf{S} \cdot \delta\mathbf{v}_{ij} - 2\mathbf{Q} \cdot \delta\mathbf{r}_{ij}, \quad (10)$$

$$\delta\mathbf{V}'_{ij} = \delta\mathbf{V}_{ij}, \quad (11)$$

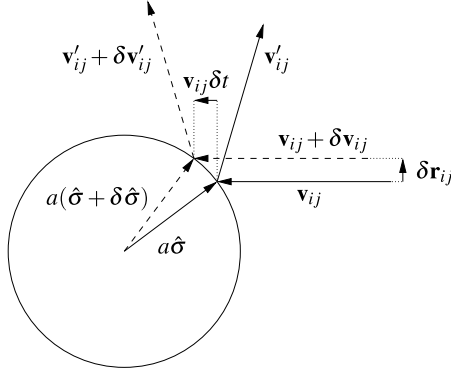


Figure 1. Two particles in a collision in relative coordinates. The collision normal $\hat{\sigma}$ is the unit vector pointing from the center of one particle to the center of the other.

in which S and Q are the $d \times d$ matrices

$$S = \hat{\sigma} \hat{\sigma}, \quad (12)$$

$$Q = \frac{[(\hat{\sigma} \cdot \mathbf{v}_{ij}) \mathbf{1} + \hat{\sigma} \mathbf{v}_{ij}] \cdot [(\hat{\sigma} \cdot \mathbf{v}_{ij}) \mathbf{1} - \mathbf{v}_{ij} \hat{\sigma}]}{a(\hat{\sigma} \cdot \mathbf{v}_{ij})}, \quad (13)$$

where $\mathbf{v}_{ij} = \mathbf{v}_i - \mathbf{v}_j$. Here the notation $\mathbf{a}\mathbf{b}$ denotes the standard tensor product of vectors \mathbf{a} and \mathbf{b} . Note that Q transforms vectors that are orthogonal to \mathbf{v}_{ij} into vectors that are orthogonal to \mathbf{v}'_{ij} . The vector \mathbf{v}_{ij} is a right zero eigenvector of Q , and \mathbf{v}'_{ij} a left zero eigenvector. Equations (7) through (13) determine $M_{\gamma_0}(t)$.

3. The radius of curvature tensor

Of particular interest for the Kolmogorov–Sinai entropy is the radius of curvature tensor, as the former is equal to the time average of the trace of the latter’s inverse. Let $\delta \mathbf{r}$ and $\delta \mathbf{v}$ represent the full dN -dimensional position and velocity perturbations respectively of all particles. The inverse radius of curvature tensor, $\mathcal{T}(t)$, is defined [4, 8, 9, 25, 26] as the inverse of the radius of curvature matrix³. It satisfies

$$\delta \mathbf{v}(\mathbf{t}) = \mathcal{T}(t) \cdot \delta \mathbf{r}(\mathbf{t}), \quad (14)$$

resulting from some, almost arbitrary, initial $\mathcal{T}(0)$ ⁴.

3.1. KS entropy and the inverse ROC tensor

To establish the relationship between the KS entropy and the trace of the inverse radius of curvature tensor we consider the time evolution over long times of the projection onto $\delta \mathbf{r}$ space of the infinitesimal volume evolving from an initial volume in tangent space spanned

³ As was noted already in [4], the radius of curvature tensor has the dimension of time, rather than length. However, it can be given the latter dimension by multiplying it by $V \equiv \sqrt{\sum_i |v_i|^2}$, which in the absence of an external potential is constant for hard spheres or disks.

⁴ It can be shown that for almost all choices of $\mathcal{T}(0)$, $\mathcal{T}(t)$ rapidly becomes independent of $\mathcal{T}(0)$ with increasing t .

A radius of curvature approach to the Kolmogorov–Sinai entropy of dilute hard particles in equilibrium

by $\delta\mathbf{r}(0)$ and $\delta\mathbf{v}(0)$. Since the projections of all Lyapunov eigenvectors with positive exponents onto $\delta\mathbf{r}$ space are linearly independent, the size of this projected volume will grow roughly as the exponent of the sum of the positive Lyapunov exponents. A more precise statement is

$$\lim_{t \rightarrow \infty} \frac{1}{t} \ln \frac{\text{vol } \delta\mathbf{r}(t)}{\text{vol } \delta\mathbf{r}(0)} = \sum_{\lambda_i > 0} \lambda_i. \quad (15)$$

Here $\text{vol } \delta\mathbf{r}(\mathbf{t})$ denotes the volume of the projection onto $\delta\mathbf{r}$ space of the evolving infinitesimal volume in tangent space. Additionally, we have the identity

$$\delta\mathbf{v}(\mathbf{t}) = \frac{d\delta\mathbf{r}(\mathbf{t})}{dt}, \quad (16)$$

which holds, except at the instants of collisions t_i , when $\delta\mathbf{r}$ is reflected in a volume-preserving unitary transformation \mathcal{U}_i . Together with equation (14), one obtains

$$\begin{aligned} \text{vol } \delta\mathbf{r}(\mathbf{t}) &= \text{vol} \left(\prod_i \mathcal{U}_i \lim_{\Delta t \rightarrow 0} \prod_{n=t_{i-1}/\Delta t}^{t_i/\Delta t - 1} (1 + \mathcal{T}(n \Delta t) \Delta t) \delta\mathbf{r}(\mathbf{0}) \right) \\ &= \prod_i \det \mathcal{U}_i \lim_{\Delta t \rightarrow 0} \prod_{n=t_{i-1}/\Delta t}^{t_i/\Delta t - 1} \det(1 + \mathcal{T}(n \Delta t) \Delta t), \end{aligned} \quad (17)$$

where the first product is over the sequence of all collisions and we employ the convention $\prod_{i=1}^n a_i \equiv a_n \cdots a_1$. This leads to

$$\lim_{t \rightarrow \infty} \frac{1}{t} \log \frac{\text{vol } \delta\mathbf{r}(\mathbf{t})}{\text{vol } \delta\mathbf{r}(\mathbf{0})} = \langle \text{Tr} \mathcal{T} \rangle. \quad (18)$$

By comparing equations (15) and (18) one obtains the desired identity⁵

$$h_{\text{KS}} = \langle \text{Tr} \mathcal{T} \rangle. \quad (19)$$

Within the framework of this article, this identity is very central. It relates the trace of the inverse radius of curvature tensor directly to the Kolmogorov–Sinai entropy, which we wish to calculate.

The rest of this paper is therefore dedicated to the description of the eigenvalues of the inverse radius of curvature tensor. We will consider their dynamics and derive approximate equations for the time evolution of their distribution. Using these we will calculate the changes in the distribution of the eigenvalues due to both free streaming and collisions. From this we obtain approximations for the stationary distribution of eigenvalues.

This calculation is simplified appreciably by restriction to low densities. We may assume then that in each collision the elements of the precollisional inverse ROC tensor involving either of the colliding particles are small, due to their decrease during the free flight preceding the collision. This assumption is violated only in collisions where one of the colliding particles has collided shortly before. The fraction of all collisions where this is the case decreases linearly with density.

⁵ Although this equation can easily be obtained from the literature [4, 21], we are not aware of it being presented in this particular form anywhere.

In section 4 two simple approximation schemes will be presented, based on the dynamics describing the changes in the distribution of eigenvalues of the inverse ROC tensor resulting from collisions.

3.2. Dynamics of the inverse radius of curvature tensor

At a given collision, between particles labeled i and j , let \mathcal{S} and \mathcal{Q} be the $dN \times dN$ -dimensional matrices which perform the transformations of $2\mathcal{S}$ and $-2\mathcal{Q}$ on the relative components in tangent space of the colliding particles and act as zero on all other independent components of $\delta\mathbf{v}$ or $\delta\mathbf{r}$, as is described in equations (8)–(11). Note that $\mathcal{Q} \cdot (\mathcal{I} - \mathcal{S})$, where \mathcal{I} is the $dN \times dN$ identity matrix, has $d - 1$ non-zero eigenvalues and is symmetric. One of the non-zero eigenvalues of $\mathcal{Q} \cdot (\mathcal{I} - \mathcal{S})$ is equal to

$$\xi_0 = -\frac{2v_{ij}}{a\hat{\mathbf{v}}_{ij} \cdot \hat{\boldsymbol{\sigma}}}, \quad (20)$$

with $\hat{\mathbf{v}}_{ij}$ the unit vector in the direction of \mathbf{v}_{ij} . The corresponding eigenvector has components in the subspaces belonging to the colliding particles of $\mathbf{e}_i = -\mathbf{e}_j = \hat{\boldsymbol{\sigma}}_{ij} - (\hat{\boldsymbol{\sigma}}_{ij} \cdot \hat{\mathbf{v}}'_{ij})\hat{\mathbf{v}}'_{ij}$ and $\mathbf{e}_k = 0$ for $k \neq i, j$ along the directions of the other particles. For $d > 2$ the other $d - 2$ non-zero eigenvalues are given by

$$\xi_0 = -\frac{2\mathbf{v}_{ij} \cdot \hat{\boldsymbol{\sigma}}}{a}, \quad (21)$$

with the eigenvector with components $\mathbf{e}_i = -\mathbf{e}_j$ normal to both $\hat{\mathbf{v}}_{ij}$ and $\hat{\boldsymbol{\sigma}}$ and again $\mathbf{e}_k = 0$. The dynamics of the inverse radius of curvature tensor at a collision can be derived by expressing $\delta\mathbf{v}'$ in terms of $\delta\mathbf{r}'$,

$$\delta\mathbf{v}' = (\mathcal{I} - \mathcal{S}) \cdot \delta\mathbf{v} + \mathcal{Q} \cdot \delta\mathbf{r} \quad (22)$$

$$= [(\mathcal{I} - \mathcal{S}) \cdot \mathcal{T} \cdot (\mathcal{I} - \mathcal{S})^{-1} + \mathcal{Q} \cdot (\mathcal{I} - \mathcal{S})^{-1}] \delta\mathbf{r}'. \quad (23)$$

With $(\mathcal{I} - \mathcal{S})^{-1} = (\mathcal{I} - \mathcal{S})$, we find for the inverse radius of curvature tensor after the collision,

$$\mathcal{T}' = (\mathcal{I} - \mathcal{S}) \cdot \mathcal{T} \cdot (\mathcal{I} - \mathcal{S}) + \mathcal{Q} \cdot (\mathcal{I} - \mathcal{S}). \quad (24)$$

The dynamics during free flight follow from (14) as

$$\mathcal{T}(t + dt) = [\mathcal{T}(t)^{-1} + \mathcal{I} dt]^{-1}. \quad (25)$$

The eigenvectors of \mathcal{T} do not change during a free flight, so its time evolution may be specified by the evolution of its eigenvalues ξ . From equation (25) one finds that these satisfy

$$\xi'(t) = -\xi(t)^2 \quad (26)$$

with solution

$$\xi(t) = \frac{1}{\xi^{-1}(0) + t}. \quad (27)$$

Note that this may be simplified by considering the dynamics of the radius of curvature tensor, \mathcal{T}^{-1} . For this operator, the drift velocity becomes a constant, 1, irrespective of the eigenvalue and the choice of time unit. However, in this case the evaluation of equation (24) becomes more complicated.

3.3. The eigenvalue distribution at low densities

At low densities the mean free-flight time is given by

$$\bar{\tau} \equiv 1/\bar{\nu} = \frac{a\Gamma(d/2)}{v_0 2n^* \pi^{(d-1)/2}}, \quad (28)$$

with $v_0 = (k_B T/m)^{1/2}$ the thermal velocity and $n^* = na^d$. The probability of a particle colliding within a free-flight time of order a/v_0 (this is the typical order of $\xi^{-1}(0)$) is of order n^* and these events, to a first approximation, may be neglected.

Let us denote a spanning set of the subspace spanned by the eigenvectors with non-zero eigenvalues of $\mathcal{Q} \cdot (\mathcal{I} - \mathcal{S})$ for a specific collision as ϵ_1 through ϵ_{d-1} . Because $\mathcal{Q} \cdot (\mathcal{I} - \mathcal{S})$ is symmetric, these vectors are both right and left eigenvectors. The corresponding eigenvalues to linear order in n^* are given by

$$\xi = \epsilon_i \cdot [(\mathcal{I} - \mathcal{S}) \cdot \mathcal{T} \cdot (\mathcal{I} - \mathcal{S}) + \mathcal{Q} \cdot (\mathcal{I} - \mathcal{S})] \cdot \epsilon_i, \quad (29)$$

$$\approx \epsilon_i \cdot [\mathcal{Q} \cdot (\mathcal{I} - \mathcal{S})] \cdot \epsilon_i, \quad (30)$$

since the elements of \mathcal{T} connecting these eigenvectors on average are of order n^* compared to the elements of $\mathcal{Q} \cdot (\mathcal{I} - \mathcal{S})$.

Under the approximation of equation (30) the vectors ϵ_i only depend on the collision parameters \hat{v}_{ij} and $\hat{\sigma}$, as specified below equations (20) and (21). The remaining eigenvalues of \mathcal{T}' , to leading order in n^* , can be identified as the eigenvalues of the projection \mathcal{PTP} of the matrix \mathcal{T} onto the $dN - d + 1$ -dimensional space orthogonal to the $d - 1$ eigenvectors ϵ_i , as follows from standard perturbation theory. Hence it follows that they are interspersed between the precollisional eigenvalues. This is worked out in appendix A.

These eigenvalues are distributed in roughly the same way as the eigenvalues of the full matrix \mathcal{T} [27, 28]. But, as the eigenvalues of \mathcal{PTP} lie in between those of \mathcal{T} , the distribution of these eigenvalues is slightly narrower than that of the eigenvalues of \mathcal{T} . For more details on this see appendix B.

In section 4, we present two approximation schemes. In the first scheme, the narrowing will be ignored and the approximation will be made that the distribution of eigenvalues of \mathcal{PTP} is the same as that of \mathcal{T} . The resulting equation for the distribution of eigenvalues can be solved analytically. Its solution is expressed in terms of the distribution $f_0(\xi_0)$ of the non-zero eigenvalues of $\mathcal{Q} \cdot (\mathcal{I} - \mathcal{S})$.

In the second scheme, a somewhat more refined approximation is made, in which we assume that each eigenvector that is changed significantly by the collision, but not created in it, can be written as a linear combination of exactly two precollisional eigenvectors. Why this is an improvement will be argued in the discussion, where we will also briefly discuss possibilities for further improvements.

4. The distribution of eigenvalues of the inverse radius of curvature tensor

4.1. The first approximation scheme

Now that the dynamics of the eigenvalues of the inverse radius of curvature tensor are specified, we may write down approximate time-evolution equations for the distribution

of these eigenvalues, $f(\xi, t)$, which is normalized to unity. Let $f_0(\xi)$ be the distribution of non-zero eigenvalues of $\mathcal{Q} \cdot (\mathcal{I} - \mathcal{S})$, which follows from equations (20) and (21) and the distribution of the collision parameters \mathbf{v}_{ij} and $\hat{\boldsymbol{\sigma}}$. We equally normalize it to unity. The simplest approximation for the rate of change of the distribution of eigenvalues of the inverse radius of curvature tensor is the one announced at the end of section 3: after a collision, the new distribution of eigenvalues is the same as the old one, except for the contributions from the non-zero eigenvalues of $\mathcal{Q} \cdot (\mathcal{I} - \mathcal{S})$. Combining this with the rate of change resulting from free streaming, one obtains

$$\frac{d}{dt}f(\xi, t) = \frac{\bar{\nu}(d-1)}{2d} [f_0(\xi) - f(\xi, t)] + \frac{\partial}{\partial \xi} [\xi^2 f(\xi, t)], \quad (31)$$

where the single-particle collision frequency is given at low density by equation (28). The first term on the right-hand side is due to collisions. The first part of it is the gain. The second part is the loss. Its form here is based on our approximation that the shape of the distribution of the remaining eigenvalues is not changed in a collision. The final term is due to the drift during free flight.

For time going to infinity, the distribution of eigenvalues becomes stationary. In other words, the left-hand side of equation (31) becomes zero. Equation (31) then may be rewritten in a more convenient form, as

$$f_0(\xi) = f_{\text{stat}}(\xi) - c \left[\xi^2 \frac{\partial}{\partial \xi} f_{\text{stat}}(\xi) + 2\xi f_{\text{stat}}(\xi) \right], \quad (32)$$

where

$$c = \frac{2d}{(d-1)\bar{\nu}}. \quad (33)$$

Solutions to this equation are of the form

$$f_{\text{stat}}(\xi) = \int_{\xi}^{\infty} d\xi_0 f_0(\xi_0) \frac{1}{c\xi^2} \exp\left(\frac{\xi - \xi_0}{c\xi_0\xi}\right). \quad (34)$$

Notice that for ξ small, as a consequence of equation (20), this reduces to $f_{\text{stat}}(\xi) = (\text{const}/c\xi^2) \exp(-1/c\xi)$.

From equation (19) it follows that the KS entropy may be obtained directly from the first moment of $f_{\text{stat}}(\xi)$. From equation (34) we find that

$$h_{\text{KS}} = \frac{Nd}{c} \int_0^{\infty} d\xi_0 f_0(\xi_0) \exp\left(\frac{1}{c\xi_0}\right) \Gamma\left(0, \frac{1}{c\xi_0}\right), \quad (35)$$

where $\Gamma(\cdot)$ denotes the incomplete gamma function, defined by

$$\Gamma(x, y) = \int_y^{\infty} dt t^{x-1} e^{-t} = e^{-y} \int_0^{\infty} dt (t+y)^{x-1} e^{-t}. \quad (36)$$

At low densities the collision frequency is low, so c is very large and the product $\exp(1/(c\xi_0))\Gamma(0, 1/(c\xi_0))$, up to corrections of $O(n)$, is equal to $\ln(c\xi_0) - \gamma$, where $\gamma \approx 0.577\,216$ is Euler's constant. The Kolmogorov–Sinai entropy then becomes

$$h_{\text{KS}} \approx \frac{N\bar{\nu}(d-1)}{2} \left\{ \left\langle \ln \frac{\xi_0}{\bar{\nu}} \right\rangle + \ln \left[\frac{2d}{(d-1)} \right] - \gamma \right\}. \quad (37)$$

We note that here the brackets, instead of a time average, denote an average over the probability distribution for the new eigenvalues at a collision, in this case f_0 . This can be expressed in terms of the joint probability distribution of the collision parameters as

$$\begin{aligned} \langle g(\xi_0) \rangle &= \int_0^\infty d\xi_0 f_0(\xi_0) g(\xi_0) = \sqrt{\frac{\beta m}{\pi^{d-1}}} \Gamma\left(\frac{d}{2}\right) \int d\mathbf{v}_i d\mathbf{v}_j d\hat{\boldsymbol{\sigma}} \theta(-\hat{\mathbf{v}}_{ij} \cdot \hat{\boldsymbol{\sigma}}) |(\mathbf{v}_i - \mathbf{v}_j) \cdot \hat{\boldsymbol{\sigma}}| \\ &\quad \times \phi_M(\mathbf{v}_i) \phi_M(\mathbf{v}_j) \frac{1}{d-1} \left[g\left(\frac{-2v_{ij}}{a\hat{\mathbf{v}}_{ij} \cdot \hat{\boldsymbol{\sigma}}}\right) + (d-2)g\left(\frac{-2\mathbf{v}_{ij} \cdot \hat{\boldsymbol{\sigma}}}{a}\right) \right], \end{aligned} \quad (38)$$

where equations (20) and (21) have been substituted and $\phi_M(\mathbf{v})$ is the Maxwell distribution,

$$\phi_M(\mathbf{v}) = \left(\frac{2\pi k_B T}{m}\right)^{-d/2} \exp\left(-\frac{m|\mathbf{v}|^2}{2k_B T}\right). \quad (39)$$

The function $\theta(x)$ is the unit step function, which vanishes for $x < 0$ and equals unity for $x \geq 0$. In general, time averages of functions of ξ may be expressed as averages over f_{stat} .

In section 5 the results from equation (37) will be discussed and compared with results from molecular dynamics simulations.

4.2. The second approximation scheme

In section 4.1, the distribution of eigenvalues after a collision was assumed to be the same as the one before, except for the non-zero eigenvalues of $\mathcal{Q} \cdot (\mathcal{I} - \mathcal{S})$. In appendix A it is shown that in reality these eigenvalues are determined by the equation

$$\sum_i \frac{c_i^2}{\xi - \xi_i} = 0, \quad (40)$$

at least in the case of $d = 2$, when $\mathcal{Q} \cdot (\mathcal{I} - \mathcal{S})$ has a single non-zero eigenvector⁶ $\boldsymbol{\epsilon}$, which can be expressed in terms of precollisional eigenvectors ψ_i of \mathcal{T} with eigenvalues ξ_i , as $\boldsymbol{\epsilon} = \sum_i c_i \psi_i$. From equation (40) one sees that precisely one new eigenvalue ξ originates between each subsequent pair of precollisional ones.

We can divide the c_i into two categories, appreciable and almost vanishing. In a pragmatic way, this distinction can be made by considering as appreciable the set of largest c_i^2 that sum to all but a small fraction of unity (for instance 0.01). The other c_i^2 , then, are almost vanishing. Due to the locality of the interactions, one may argue that, in the limit of a large system, the number of appreciable c_i is small compared to N in most cases.

For eigenvectors with very small values of c_i a new eigenvalue is found very close to an old one, typically to the left or right of the old one if the nearest eigenvalue with appreciable c_i is to the left respectively to the right of ψ_i . This may be interpreted in the following way: in equation (40) one may ignore all eigenvectors with almost vanishing c_i , because their forms and eigenvalues remain essentially unchanged. For the remaining eigenvalues one retains the property that new eigenvalues are interspersed between the old ones. This is illustrated in figure 2.

⁶ The generalization to the case of more than one non-zero eigenvector is also discussed in appendix A.

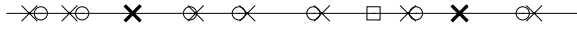


Figure 2. An impression of eigenvalues on an interval. The crosses denote precollisional eigenvalues, the circles and squares postcollisional ones. The bold and the regular crosses denote eigenvalues corresponding to eigenvectors with an appreciable and almost vanishing c_i^2 respectively. The circles and square denote new eigenvalues. The eigenvalue indicated by the square is approximately the solution of equation (40) with only the eigenvalues with appreciable c_i^2 , indicated with bold crosses, contributing. The circles almost coincide with precollisional eigenvalues with almost vanishing c_i^2 .

The number of eigenvectors contributing appreciably to equation (40) varies from collision to collision, but it is always at least 2, because the two colliding particles cannot have collided before without intermediate collisions with other particles. The actual distribution of the number of contributing eigenvectors and the distribution of the values of the corresponding c_i are not easy to determine. In this subsection we make two simplifying assumptions: firstly, that the number of contributing eigenvectors is always just 2 and, secondly, that their coefficients c_1 and c_2 are distributed isotropically, irrespective of the eigenvalues ξ_1 and ξ_2 . This means that these coefficients can be represented as $c_1 = \cos \phi$ and $c_2 = \sin \phi$, with ϕ distributed uniformly on the unit circle. This assumption implies that the distribution of the corresponding original eigenvalues ξ_1 and ξ_2 is the same as the (as yet unknown) overall distribution of eigenvalues of the inverse radius of curvature tensor. Obviously, these assumptions are at best approximately correct, but in our discussion we will make it plausible, on the basis of these assumptions, that a better approximation can be obtained for the eigenvalue distribution than the one given in equation (34).

At a collision, the two eigenvalues ξ_1 and ξ_2 disappear and are replaced by a new eigenvalue, ξ_0 , related to $\mathcal{Q} \cdot (\mathcal{I} - \mathcal{S})$, and the mixed eigenvalue

$$\xi = \xi_1 c_2^2 + \xi_2 c_1^2, \tag{41}$$

as follows from equation (40). The eigenvector belonging to this mixed eigenvalue is a linear combination of the two old eigenvectors, orthogonalized to the non-zero eigenvectors of $\mathcal{Q} \cdot (\mathcal{I} - \mathcal{S})$. Under these approximations the collision term in equation (31) is modified, leading to

$$\frac{d}{dt} f(\xi, t) = \frac{\bar{v}(d-1)}{2d} [f_0(\xi) + f_{\text{coll}}[f](\xi, t) - 2f(\xi, t)] + \frac{\partial}{\partial \xi} [\xi^2 f(\xi, t)], \tag{42}$$

where $f_{\text{coll}}[f](\xi, t)$ represents the distribution of the new mixed eigenvalue after the collision, as a functional of $f(\xi, t)$, the distribution before the collision.

Under the assumptions described above this distribution can be written as

$$f_{\text{coll}}[f](\xi, t) = \int \int d\xi' d\xi'' f(\xi', t) f(\xi'', t) h(\xi | \xi', \xi''). \tag{43}$$

Here $h(\xi|\xi', \xi'')$ is the distribution of the new eigenvalue ξ between the eigenvalues ξ' and ξ'' . The function h assumes the form

$$h(\xi, |\xi', \xi'') = \frac{1}{\pi \sqrt{(\xi - \xi')(\xi'' - \xi)}}. \quad (44)$$

From this an equation similar to equation (32) can be derived. One finds

$$f_0(\xi) = 2f_{\text{stat}}(\xi) - f_{\text{coll}}[f_{\text{stat}}](\xi) - c \left[\xi^2 \frac{\partial}{\partial \xi} f_{\text{stat}}(\xi) + 2\xi f_{\text{stat}}(\xi) \right]. \quad (45)$$

This equation can easily be solved numerically and from its solution a second prediction of h_{KS} can be obtained. These results are discussed in section 5.

5. Results and discussion

In the previous sections we have developed two closely related analytical schemes that enable us to calculate approximations for the stationary distribution of eigenvalues of the inverse radius of curvature tensor. From this distribution we may obtain expressions for the leading order terms in the density expansion of the KS entropy of a gas of hard disks or spheres. In particular, the predictions resulting from equation (34) and numerical solutions of equation (45) may be compared to the results of [11, 21] and results from molecular dynamics simulations.

In [11] Van Beijeren *et al* proposed as the approximation for the KS entropy

$$h_{\text{KS}}^{(0)} \approx \frac{N\bar{\nu}(d-1)}{2} \left\langle \ln \xi_0 + \ln \left(\frac{\tau_i + \tau_j}{2} \right) \right\rangle, \quad (46)$$

with τ_i the free-flight time of particle i since the previous collision. Putting this in the form of equation (1) leads to $A = (d-1)/2$ and, after numerical integration,

$$B^{(0)} \approx \begin{cases} 0.209 & \text{if } d = 2 \\ -0.583 & \text{if } d = 3. \end{cases} \quad (47)$$

From molecular dynamics simulations, Posch and co-workers [11, 29] found the following results for the Kolmogorov–Sinai entropy at low densities:

$$h_{\text{KS}}^{\text{num.}} = \begin{cases} (0.499 \pm 0.001)N\bar{\nu} (-\ln na^d + 1.366 \pm 0.005) & \text{if } d = 2 \\ (1.02 \pm 0.02)N\bar{\nu} (-\ln na^d + 0.29 \pm 0.01) & \text{if } d = 3. \end{cases} \quad (48)$$

Comparing the results of equation (37) to those of [11], equation (46), we find that A is the same, but for B one obtains corrections to equation (47) of the form

$$\Delta B = \ln \left(\frac{2d}{d-1} \right) - \gamma - \left\langle \ln \left[\frac{\bar{\nu}(\tau_i + \tau_j)}{2} \right] \right\rangle. \quad (49)$$

Dorfman *et al* already anticipated corrections of $\ln 4 \approx 1.386$ for $d = 2$ and $\ln 3 \approx 1.098$ for $d = 3$ [30], corresponding to the first term in equation (49).

In [21], elements of the radius of curvature matrix were estimated by considering the stretching of the tangent phase space during a sequence of two collisions with free flights; it was estimated that

$$B^{\text{dW}} = \begin{cases} 1.47 \pm 0.11 & \text{if } d = 2 \\ 0.35 \pm 0.08 & \text{if } d = 3. \end{cases} \quad (50)$$

We have evaluated the averages in equation (49) by integrating over the joint distribution of the collision parameters (see equation (38)). The values for the parameter B resulting from the first approximation scheme follow as

$$B^{(1)} = \begin{cases} 2 - \frac{3}{2}\gamma + \ln 2 - \frac{1}{2} \ln \pi \approx 1.255 & \text{if } d = 2 \\ \frac{1}{2} - \frac{3}{2}\gamma + \ln 3 - \frac{1}{2} \ln \pi \approx 0.160 & \text{if } d = 3. \end{cases} \quad (51)$$

These results are in reasonable agreement with the results from the molecular dynamics simulations [29], given in equation (48).

More accurate results can be obtained from the second approximation scheme by numerically solving equation (45). The solution for $f_{\text{stat}}(\xi)$ for $d = 2, n = 0.001$ is displayed in figure 4. From this, one finds an additional correction to B of

$$\Delta B = 0.086, \quad (52)$$

regardless of the dimensionality. This leads to a final result for the constant B of

$$B^{(2)} \approx \begin{cases} 1.341 & \text{if } d = 2 \\ 0.247 & \text{if } d = 3. \end{cases} \quad (53)$$

This is in good agreement with the results from the molecular dynamics simulations, and in particular also in better agreement than the results of [21], equation (50).

5.1. Comparing approximation schemes

We now argue as to why the distribution of inverse radius of curvature tensor eigenvalues obtained from the two-eigenvalue approximation resulting in equation (42) can be expected to be better than the simpler approximation, equation (31), resulting from assuming the distribution of interspersed new eigenvalues to be the same as that of the precollisional eigenvalues. Consider the first two moments of these distributions. In the simple approximation these are not changed from their precollisional values. Therefore, as mentioned already, the spectrum does not exhibit any narrowing in collisions, as it should according to the arguments presented before, which are supported by the calculations presented in appendix B. In the two-eigenvalue approximation, two eigenvalues ξ_1 and ξ_2 are sampled independently from the stationary distribution and replaced by one interspersed eigenvalue with the value $\xi' = \xi_1 c_2^2 + \xi_2 c_1^2$, according to equation (41). The other interspersed eigenvalues retain their precollisional values. The coefficients c_1 and c_2 are sampled as $c_1 = \cos \phi$ and $c_2 = \sin \phi$, with ϕ distributed uniformly on the unit circle. Hence the average value of ξ' is the same as that of the precollisional eigenvalues, as should be the case (see appendix B). From equation (41) and the assumed distribution of the c_i one also easily finds the collisional changes of the second moments. In appendix B it is shown that, to leading order in $1/n$ the average of the second moment is reduced at a collision by a factor $1 - (1 - A)/n$, with A a constant with a value between zero and unity.

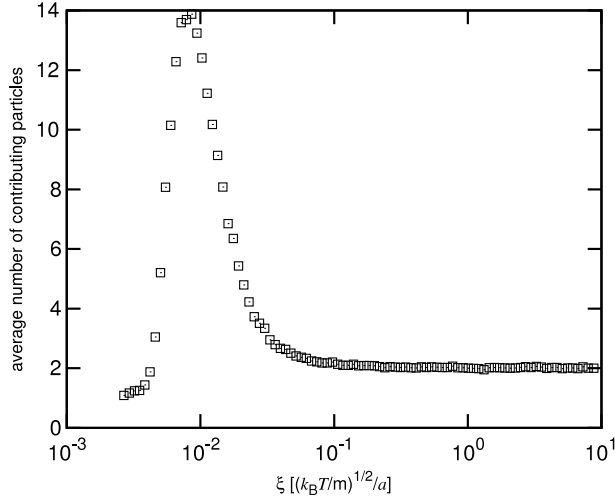


Figure 3. Eigenvalue composition, as obtained from molecular dynamics simulation of 64 two-dimensional particles at $n^* 0.01$ in a square box. The figure shows an estimate for the average number of particles which contribute significantly to an eigenvector of the inverse radius of curvature as a function of the corresponding eigenvalue ξ . This estimate is given by the ratio of the averages of the second and fourth powers of the component of the eigenvector in the subspace of a particle. The estimate is somewhat indirect, but it is clear that it is exact in the special case where the weight is distributed equally over a set of particles. At this density, the collision frequency is approximately equal to $0.0354(k_B T/m)^{1/2}/a$. In order to obtain sufficient information both at high and at low densities, non-linear binning was used. The plot only shows results for bins that contain more than 10 points.

This constant, defined in the appendix through $\sum_{i=1}^n \langle c_i^4 (\xi_i - \langle \xi \rangle)^2 \rangle = A/n \langle \sum_{i=1}^n (\xi_i - \langle \xi \rangle)^2 \rangle$, can be calculated in the two-eigenvalue approximation from the assumed distribution of c_1 and c_2 as $A_2 = 3/4$. Since in most cases the new eigenvector will be composed of more than two precollisional eigenvectors, A_2 will be an upper bound to the actual A . Hence the two-eigenvalue approximation does lead to a narrowing of the spectrum, but it underestimates its extent. This is especially true in the region where $f(\xi)$ reaches its maximum, since there the eigenfunctions of the ROC tensor tend to be carried by many particles, as one can see from figures 3 and 4.

The results may be improved, in principle, by considering larger sets of eigenvectors for spanning the ϵ_i . However, to do this in a sensible way one would need the distribution of the c_i , preferably as a function of all ξ_i . So far no theory has been developed for this and it seems no simple task to do so. One could of course study this distribution numerically, but that would bring one close already to a full numerical study of the eigenvalue spectrum of the inverse radius of curvature tensor.

In figure 3 we plot numerical results for the average number of particles contributing to an eigenvalue as a function of ξ , in a system of 64 two-dimensional particles in a square box with periodic boundary conditions. For ξ larger than the collision frequency, most eigenvectors are carried by two particles, indicating that these are new eigenvectors ϵ_i . For smaller ξ there is a rapid increase in the average number of particles carrying an

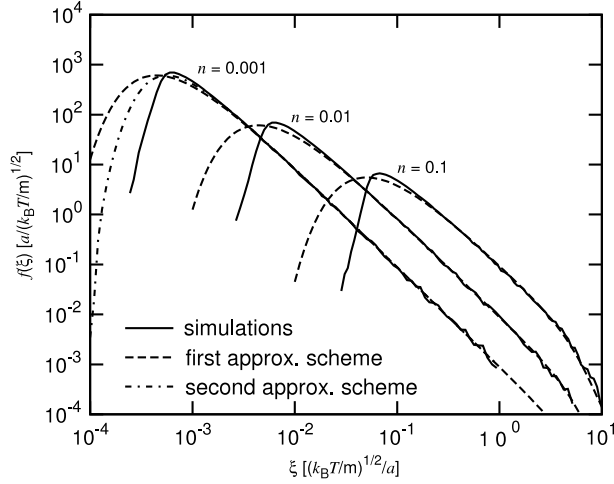


Figure 4. The distribution of eigenvalues of the inverse radius of curvature tensor for $d = 2$ as calculated in this paper compared to results from simulations for various densities. Dashed and dot–dashed lines show the results of the present calculations, while solid lines represent the values found in the simulations. The results for the second approximation scheme are only shown for $n^* = 0.001$, for which we calculated them with great accuracy. Similar curves would be obtained at the other densities. The simulated systems consist of 64 particles in square boxes with periodic boundary conditions. Runs were performed of 100 000 collisions, and the eigenvalues of the radius of curvature were calculated and binned every 64 collisions. In order to obtain sufficient information both at high and at low densities, non-linear binning was used. The plot only shows results for bins that contain more than 10 points.

eigenvector, followed by a sharp drop below $\xi \approx 0.25\nu \approx 0.9 \times 10^{-2}(k_B T/m)^{1/2}/a$. The eigenvectors corresponding to smaller eigenvalues have drifted for a long time, during which in most cases the particles contributing to them have collided many times. These eigenvectors are therefore typically carried by more particles. But, remarkably, for very low eigenvalues the number of particles carrying the eigenvector becomes very close to 1. This is related to the existence of particles that have not collided for several mean free times. As a result of subsequent projections normal to new eigenvectors, the weight of such a particle in the remaining eigenvector can increase from the original value $1/2$ to values close to unity. The contribution of these eigenvectors to the KS entropy is very small.

We cannot directly translate the data of figure 3 to an estimate of the number of eigenvectors contributing significantly to a newly generated eigenvector ϵ_i . It is clear though that there is a strong correlation. Since the new ϵ_i are always carried by just the two colliding particles, the components along them of eigenvalues carried by several particles necessarily have to be small. Hence, many of these are required to reconstruct any given ϵ_i .

Another, more technical approach was based on a calculation of the distribution of elements of the radius of curvature [21, 31]. The results in the present paper are more accurate than the results of that calculation, and were obtained in a more elegant way.

On the other hand, it is not directly clear to us how to further improve the accuracy of the calculation presented here, nor if the distribution of eigenvalues of the radius of curvature could be used to calculate specific Lyapunov exponents of the system, as can be done with the distribution of the elements of the radius of curvature [22].

5.2. The distribution of eigenvalues from a simulation

In our present calculation of the Kolmogorov–Sinai entropy of a dilute hard-sphere gas the central quantity to be computed is the stationary distribution of eigenvalues of the inverse radius of curvature tensor. It is interesting to compare the calculated distribution to results from computer simulations. We have performed MD simulations for a system of hard disks, in which we calculated the radius of curvature tensor from the numerical values of $\delta\mathbf{r}$ and $\delta\mathbf{v}$ by making use of equation (14) and diagonalized it at regular time intervals. The results of these simulations are displayed in figure 4, along with the theoretical predictions. For a large range of eigenvalues, the calculations follow the simulations closely, including at very high ξ . At the lowest values of the range studied, there appear some differences.

It can be seen from figure 4 that the small eigenvalues have a more peaked, and hence narrower distribution than was found from the calculations. This is due to the fact that only linear combinations of two eigenvectors were considered for ϵ_i . In fact, as can be seen from figure 3 eigenvectors near the peak are generally carried by more particles and their contribution to ϵ_i , which is carried by only two particles, will therefore have a small coefficient c_i . As argued above, the larger the number of particles carrying an eigenvector, the smaller the value of A and the stronger the narrowing. And equation (40) reveals that for given ξ the dynamics are dominated by nearby eigenvalues and their c_i . As can be seen from figure 4, the distribution calculated using linear combinations of two eigenvectors not only predicts the KS entropy better than the approximation based on no change in the spectrum of interspersed eigenvalues, but also follows the simulation results more closely for intermediate eigenvalues.

6. Conclusions

In this paper we have calculated the Kolmogorov–Sinai entropy of systems consisting of hard disks or spheres from the stationary distribution of the eigenvalues of the inverse radius of curvature tensor. The dynamics of these eigenvalues consist of free streaming and collisional effects. The latter are a combination of the generation of new eigenvalues, with a well-defined distribution, and a slight narrowing of the spectrum of remaining eigenvalues with respect to the precollisional spectrum. A simple approximation, which ignores this narrowing and assumes the spectrum to remain unchanged at collisions on average, already reproduces the numerically observed spectrum quite well, with a fairly accurate prediction of the KS entropy. A slightly more refined approximation, assuming that the new eigenvectors consist of just two precollisional ones, both sampled randomly from the full distribution, does predict a narrowing of the spectrum at collisions, though it underestimates its extent. This approximation gives quite accurate results for the KS entropy and it reproduces the eigenvalue spectrum of the inverse radius of curvature tensor better than the simplest approximation. The remaining underestimation of the narrowing is strongest and most clearly visible at small eigenvalues.

In order to improve on the estimates developed here one needs more knowledge on the decomposition of the new eigenvectors created in a collision into precollisional eigenvectors. This is highly non-trivial, however.

It should be noted that, though the specific dynamics of the inverse radius of curvature tensor are different for other high-dimensional systems, such as the high-dimensional Lorentz gas [12] (which has uniformly convex scatterers), their overall behavior is generic for all systems consisting of many particles.

Describing the dynamics of the eigenvalues of the inverse radius of curvature tensor by means of a Fokker–Planck equation seems an attractive approach. In order to do this one needs expressions for the local drift and diffusion of the eigenvalues due to collisions. For this again more knowledge is needed of the way new eigenvectors are composed from old ones. Furthermore, the Fokker–Planck equation is a good approximation for systems where the dynamics consist of small jumps, while in the present case, large jumps also happen. However, these will mostly occur for large values of ξ , where the dynamics is dominated by the drift. Therefore the Fokker–Planck equation may still be a good approximation.

Finally, the expressions derived here for the dynamics of the inverse radius of curvature tensor, and the equations for the distribution of its eigenvalues, equations (31) and (42), can also be used for systems in a stationary non-equilibrium state. In such a state, the distributions of velocities and collision parameters are different and one has to take this into account when calculating the averages or the source terms in equations (31) and (42).

Acknowledgments

ASdW’s work was financially supported by a Veni grant from the Netherlands Organisation for Scientific Research (NWO). HvB acknowledges support by the Humboldt Foundation. This work was also supported by the Foundation for Fundamental Research on Matter (FOM), which is financially supported by NWO.

Appendix A. Eigenvalues of a submatrix

Let \mathcal{P}_1 through \mathcal{P}_{d-1} be the projection operators which project out the $d-1$ orthogonal unit vectors ϵ_1 through ϵ_{d-1} . We are interested in the (distribution of) non-zero eigenvalues of the submatrix $\mathcal{P}\mathcal{T}\mathcal{P}$ of a symmetric matrix \mathcal{T} , with $\mathcal{P} = \mathcal{P}_1 \cdot \dots \cdot \mathcal{P}_{d-1}$. We shall determine these by considering the non-zero eigenvalues ξ'_i of $\tilde{\mathcal{T}}' = \mathcal{P}_x \tilde{\mathcal{T}} \mathcal{P}_x$, and their corresponding eigenvectors η_i . The eigenvalues of $\mathcal{P}\mathcal{T}\mathcal{P}$ can now be determined by applying this procedure $d-1$ times, projecting subsequently normal to each of the $d-1$ non-vanishing eigenvalues of $(\mathcal{T} - \mathcal{S}) \cdot \mathcal{Q}$. Thus one obtains matrices $\tilde{\mathcal{T}}$ with a decreasing number of non-zero eigenvalues.

Let ψ_1 through ψ_z be the z normalized eigenvectors of a matrix $\tilde{\mathcal{T}}$ with corresponding eigenvalues ξ_i . Let us write the unit vector that is to be projected out, ϵ_x , and an eigenvector η of $\tilde{\mathcal{T}}'$ with eigenvalue ξ' in terms of the eigenvectors of $\tilde{\mathcal{T}}$,

$$\epsilon_x = \sum_i c_i \psi_i, \tag{A.1}$$

$$\eta = \sum_i \beta_i \psi_i, \tag{A.2}$$

with

$$\sum_i c_i^2 = \sum_i \beta_i^2 = 1. \quad (\text{A.3})$$

As η has no component along ϵ_x , we may write

$$\xi' \eta = \xi' \sum_i \beta_i \psi_i \quad (\text{A.4})$$

$$= \tilde{T}' \eta = \mathcal{P}_x \tilde{T} \eta = \mathcal{P}_x \sum_i \beta_i \xi_i \psi_i \quad (\text{A.5})$$

$$= \sum_i (\beta_i \xi_i - \mu c_i) \psi_i, \quad (\text{A.6})$$

with μ a constant such that

$$\epsilon_x \cdot \xi' \eta = \sum_i c_i (\beta_i \xi_i - \mu c_i) = 0. \quad (\text{A.7})$$

By taking the inner product of equation (A.6) with a given ψ_i one finds that

$$\beta_i = -\frac{\mu c_i}{\xi' - \xi_i}. \quad (\text{A.8})$$

By substituting equation (A.8) into (A.7), and dividing by μ and ξ' , we find that

$$\sum_i \frac{c_i^2}{\xi_i - \xi'} = 0. \quad (\text{A.9})$$

From this equation it follows directly that between each subsequent pair ξ_i and ξ_{i+1} there must be precisely one solution for ξ' .

Appendix B. Narrowing of the eigenvalue spectrum

In order to investigate the narrowing of the spectrum of eigenvalues as a result of a collision we rewrite equation (A.9), multiplying it by $-\prod_i (\xi' - \xi_i)$, and find

$$\xi'^{m-1} - \sum_i (1 - c_i^2) \xi_i \xi'^{m-2} + \sum_{i < j} (1 - c_i^2 - c_j^2) \xi_i \xi_j \xi'^{m-3} + \dots = 0, \quad (\text{B.1})$$

where we have made use of equation (A.3). By comparing the coefficient of $(\xi')^{n-2}$ to the coefficient in the eigenvalue equation for ξ' , one immediately obtains

$$\sum_{i=1}^{n-1} \xi'_i = \sum_{i=1}^n (1 - c_i^2) \xi_i. \quad (\text{B.2})$$

In section 3 we have found that the eigenvectors ϵ_z consist of equal and opposite components of two arbitrarily determined (colliding) particles along a unit vector that is distributed isotropically in d -dimensional space. From this it follows immediately that the average of c_i^2 over many collisions has to be equal to $1/n$. If in equation (B.2) we replace c_i^2 by this average we find that the mean value of the interspersed eigenvalues on

A radius of curvature approach to the Kolmogorov–Sinai entropy of dilute hard particles in equilibrium

average is the same as that of the precollisional ones. Note that equations (31) and (42) both satisfy this property.

Similarly, from the coefficient of $(\xi')^{n-2}$ one obtains the identity

$$\sum_{i < j}^{n-1} \xi'_i \xi'_j = \sum_{i < j}^n (1 - c_i^2 - c_j^2) \xi_i \xi_j. \quad (\text{B.3})$$

Combining this with equation (B.2) one finds the identity

$$\begin{aligned} \sum_{i=1}^{n-1} \langle (\xi'_i - \langle \xi \rangle)^2 \rangle &= \frac{1}{n^2} \left\langle \left(\sum_{i=1}^n (\xi_i - \langle \xi \rangle) \right)^2 \right\rangle + \left(1 - \frac{2}{n} - \frac{1}{n^2} \right) \sum_{i=1}^n \langle (\xi_i - \langle \xi \rangle)^2 \rangle \\ &+ \sum_{i=1}^n \langle c_i^4 (\xi_i - \langle \xi \rangle)^2 \rangle. \end{aligned} \quad (\text{B.4})$$

Here the brackets indicate an average over many subsequent collisions. We used the identity

$$\langle c_i^2 c_j^2 \xi_i \xi_j \rangle = \frac{1}{n^2} \langle \xi_i \xi_j \rangle \quad i \neq j, \quad (\text{B.5})$$

and we introduced the symbol $\langle \xi \rangle$ defined by

$$\langle \xi \rangle = \frac{1}{n} \left\langle \sum_{i=1}^n \xi_i \right\rangle. \quad (\text{B.6})$$

To leading order in $1/n$ the terms proportional to $1/n^2$ in equation (B.4) may be ignored. We introduce the constant A defined through

$$\sum_{i=1}^n \langle c_i^4 (\xi_i - \langle \xi \rangle)^2 \rangle = \frac{A}{n} \sum_{i=1}^n \langle (\xi_i - \langle \xi \rangle)^2 \rangle. \quad (\text{B.7})$$

Note that A is smaller than 1, since $c_i^4 < c_i^2$ and $\langle c_i^2 \rangle = 1/n$. To leading order in $1/n$, combination of equations (B.4) and (B.7) leads to the reduction factor mentioned in section 5.1. Obviously, the smaller A , the stronger the narrowing. This should apply also locally, implying stronger narrowing in regions where the eigenvectors tend to be carried by more particles.

References

- [1] Dorfman J R, 1999 *An Introduction to Chaos in Nonequilibrium Statistical Mechanics (Lecture Notes in Physics No. 14)* (Cambridge: Cambridge University Press)
- [2] Gaspard P, 1998 *Chaos, Scattering and Statistical Mechanics (Nonlinear Science Series No. 9)* (Cambridge: Cambridge University Press)
- [3] van Zon R, van Beijeren H and Dorfman J R, *Kinetic theory of dynamical systems*, 2000 *Proc. 1998 NATO-ASI Dynamics: Models and Kinetic Methods for Non-equilibrium Many-Body Systems* ed J Karkheck (Dordrecht: Kluwer) p 131
- [4] van Zon R, van Beijeren H and Dorfman J R, *Kinetic theory estimates for the Kolmogorov–Sinai entropy and the Lyapunov exponents for dilute, hard-ball gases and for dilute, random Lorentz gases*, 2000 *Hard Ball Systems and the Lorentz Gas (Encyclopedia of Mathematical Sciences)* ed D Szasz (Berlin: Springer)
- [5] Gaspard P and Nicolis G, *Transport properties, Lyapunov exponents and entropy per unit time*, 1990 *Phys. Rev. Lett.* **65** 1693

- [6] Dorfman R J and Gaspard P, *Chaotic scattering theory of transport and reaction-rate coefficients*, 1995 *Phys. Rev. E* **51** 28
- [7] Dorfman R J and Gaspard P, *Chaotic scattering theory, thermodynamic formalism, and transport coefficients*, 1995 *Phys. Rev. E* **52** 3525
- [8] van Beijeren H and Dorfman J R, *Lyapunov exponents and KS entropy for the Lorentz gas at low densities*, 1995 *Phys. Rev. Lett.* **74** 4412
van Beijeren H and Dorfman J R, 1996 *Phys. Rev. Lett.* **76** 3238 (plus erratum)
- [9] Latz A, van Beijeren H and Dorfman J R, *Lyapunov spectrum and the conjugate pairing rule for a thermostated random Lorentz gas: kinetic theory*, 1997 *Phys. Rev. Lett.* **78** 207
- [10] Dellago C and Posch H A, *Lyapunov spectrum and the conjugate pairing rule for a thermostated random Lorentz gas: numerical simulations*, 1997 *Phys. Rev. Lett.* **78** 211
- [11] van Beijeren H, Dorfman J R, Posch H A and Dellago C, *The Kolmogorov–Sinai entropy for dilute gases in equilibrium*, 1997 *Phys. Rev. E* **56** 5272
- [12] de Wijn A S and van Beijeren H, *The Lyapunov spectrum of the many-dimensional dilute random Lorentz gas*, 2004 *Phys. Rev. E* **70** 036209
- [13] Posch H A and Hirschl R, *Simulations of billiards and of hard body fluids*, 2000 *Hard Ball Systems and the Lorentz Gas (Encyclopedia of Mathematical Sciences)* vol 101, ed D Szasz (New York: Springer) p 280
- [14] Forster C, Hirschl R, Posch H A and Hoover W G, *Perturbed phase-space dynamics of hard-disk fluids*, 2004 *Physica D* **187** 294
- [15] Eckmann J-P, Forster C, Posch H A and Zabey E, *Lyapunov modes in hard-disk systems*, 2005 *J. Stat. Phys.* **118** 813 [arXiv:nlin.CD/0404007]
- [16] van Zon R, van Beijeren H and Dellago C, *Largest Lyapunov exponent for many particle systems at low densities*, 1998 *Phys. Rev. Lett.* **80** 2035
- [17] van Zon R, *Chaos in dilute hard sphere gases in and out of equilibrium*, 2000 PhD Thesis Utrecht University
- [18] van Zon R and van Beijeren H, *Front propagation techniques to calculate the largest Lyapunov exponent of dilute hard disk gases*, 2002 *J. Stat. Phys.* **109** 641
- [19] McNamara S and Mareschal M, *On the origin of the hydrodynamic Lyapunov modes*, 2001 *Phys. Rev. E* **64** 051103
- [20] de Wijn A S and van Beijeren H, *Goldstone modes in Lyapunov spectra of hard sphere systems*, 2004 *Phys. Rev. E* **70** 016207
- [21] de Wijn A S, *The Kolmogorov–Sinai entropy for dilute hard particles in equilibrium*, 2005 *Phys. Rev. E* **71** 046211
- [22] de Wijn A S, *Lyapunov spectra of billiards with cylindrical scatterers: comparison with many-particle systems*, 2005 *Phys. Rev. E* **72** 026216
- [23] Abraham R and Marsden J E, 1978 *Foundations of Mechanics* (New York: Benjamin)
- [24] Dragt A J, 1978 *Lectures on Nonlinear Orbit Dynamics* vol 87 (Woodbury, NY: American Institute of Physics)
- [25] Dellago C, Posch H A and Hoover W G, *Lyapunov instability in a system of hard disks in equilibrium and nonequilibrium steady states*, 1996 *Phys. Rev. E* **53** 1485
- [26] Sinai Ya G, 1970 *Russ. Math. Surv.* **25** 137
Bunimovich L A and Sinai Ya G, 1980 *Commun. Math. Phys.* **78** 479
Bunimovich L A, Sinai Ya G and Chernov N I, 1990 *Russ. Math. Surv.* **45** 105
Sinai Ya G and Krylov N N, 1979 *Works on the Foundations of Statistical Mechanics* (Princeton, NJ: Princeton University Press) p 239
Sinai Ya G (ed), 1991 *Dynamical Systems: Collection of Papers* (Singapore: World Scientific)
- [27] Crisanti A, Paladin G and Vulpiani A, 1993 *Products of Random Matrices in Statistical Physics* (New York: Springer)
- [28] Mehta M L, 1991 *Random Matrices* 2nd edn (San Diego, CA: Academic)
- [29] Forster C and Posch H A, 2004 private communication
- [30] Dorfman J R, Latz A and van Beijeren H, *Bogoliubov–Born–Green–Kirkwood–Yvon hierarchy methods for sums of Lyapunov exponents for dilute gases*, 1998 *Chaos* **8** 444 [arXiv:chao-dyn/9801014]
- [31] de Wijn A S, *Chaos in systems with many degrees of freedom*, 2004 PhD Thesis Utrecht University